AGU PUBLICATIONS

JGR

Journal of Geophysical Research: Atmospheres

RESEARCH ARTICLE

10.1002/2017JD027359

Key Points:
- Disagreements between major emissions inventories exceed 100% for large urban areas of the northeastern U.S.
- The Anthropogenic Carbon Emissions System (ACES) provides an improved spatial representation of urban emissions at 1 km^2 resolution
- Urban emissions comprise widely varying shares of state-level emissions, from 22% in VT to 85% in NJ

Supporting Information:
- Supporting Information S1

Correspondence to:
C. K. Gately,
cgately@gmail.com

Citation:
Gately, C. K., & Hutyra, L. R. (2017). Large uncertainties in urban-scale carbon emissions. *Journal of Geophysical Research: Atmospheres*, *122*, 11,242–11,260. https://doi.org/10.1002/2017JD027359

Received 27 JUN 2017
Accepted 8 OCT 2017
Accepted article online 12 OCT 2017
Published online 30 OCT 2017

Large Uncertainties in Urban-Scale Carbon Emissions

C. K. Gately[1,2] and L. R. Hutyra[1]

[1]Department of Earth and Environment, Boston University, Boston, MA, USA, [2]Earth and Planetary Sciences Department, Harvard University, Cambridge, MA, USA

Abstract Accurate estimates of fossil fuel carbon dioxide ($FFCO_2$) emissions are a critical component of local, regional, and global climate agreements. Current global inventories of $FFCO_2$ emissions do not directly quantify emissions at local scales; instead, spatial proxies like population density, nighttime lights, and power plant databases are used to downscale emissions from national totals. We have developed a high-resolution (hourly, 1 km^2) bottom-up Anthropogenic Carbon Emissions System (ACES) for $FFCO_2$, based on local activity data for the year 2011 across the northeastern U.S. We compare ACES with three widely used global inventories, finding significant differences at regional (20%) and city scales (50–250%). At a spatial resolution of 0.1°, inventories differ by over 100% for half of the grid cells in the domain, with the largest differences in urban areas and oil and gas production regions. Given recent U.S. federal policy pull backs regarding greenhouse gas emissions reductions, inventories like ACES are crucial for U.S. actions, as the impetus for climate leadership has shifted to city and state governments. The development of a robust carbon monitoring system to track carbon fluxes is critical for emissions benchmarking and verification. We show that existing downscaled inventories are not suitable for urban emissions monitoring, as they do not consider important local activity patterns. The ACES methodology is designed for easy updating, making it suitable for emissions monitoring under most city, regional, and state greenhouse gas mitigation initiatives, in particular, for the small- and medium-sized cities that lack the resources to regularly perform their own bottom-up emissions inventories.

1. Introduction

Global emissions of carbon dioxide from the combustion of fossil fuels ($FFCO_2$) comprise the largest net flux of carbon into the atmosphere (Intergovernmental Panel on Climate Change, 2013). However, these fluxes are highly variable across space and time, and quantifying their spatiotemporal patterns remains a challenge at subnational and subannual scales. Inventories of $FFCO_2$ emissions have been conducted at global and national scales for several decades, largely based on public reports of energy consumption published by national and international statistical agencies (Andres et al., 1996; Gregg et al., 2009; Marland et al., 1985). Higher-resolution, gridded inventories were developed soon after in order to support continental and regional modeling of the terrestrial carbon cycle (Gurney et al., 2003; Peters et al., 2007; Schuh et al., 2010). More recently, continued improvements in atmospheric measurement and modeling platforms (Lauvaux et al., 2016; McKain et al., 2014, 2012; Ogle et al., 2015; Turnbull et al., 2015; Wu et al., 2011), and a rapidly growing adoption of regional and local emissions mitigation policies, have led to a growing demand for detailed, sector-specific emissions inventories at highly resolved spatial and temporal scales (1 km^2, hourly) that cover broad domains (regional, continental) (Global Covenant of Mayors for Climate and Energy, 2016; Regional Greenhouse Gas Initiative, 2005; State of California AB-32, 2006). Although a national carbon policy will have as its ultimate goal the reduction of total emissions, achieving reductions requires policies that are designed for and implemented at state and local scales, due to the highly variable nature of the many sources of carbon emissions. Unfortunately, the United States currently lacks the ability to accurately and comprehensively measure and track changes in $FFCO_2$ emissions at local and regional scales (Gurney et al., 2015).

Detailed quantification of emissions—at all spatial scales from city to national—is necessary to inform the design, implementation, and evaluation of emissions mitigation policies across a wide range of administrative scales (city, state, regional, and national) (Ciais et al., 2014; Gurney et al., 2015). Over 600 cities, representing 445,581,500 people worldwide, have signed pledges to reduce their greenhouse gas emissions and create robust inventories of their emissions (Global Covenant of Mayors for Climate and Energy, 2016). Having sector-specific emissions estimates is vital, as state and local governments may prefer to focus on particular sectors where emissions reductions may be mandated by local policies, easier to achieve, or

more cost effective (Miller & Michalak, 2016). For example, in large urban areas city governments may have limited authority or ability to influence road sector emissions from freight or commuter traffic but can more easily enact energy efficiency policies for residential or commercial buildings.

City- and state-level emissions inventories rarely report on the within domain spatial distribution of emissions, as they are typically designed to provide aggregated emissions totals to support trend analysis and reporting requirements. However, understanding the spatial patterns of emissions within a city, and how these emissions covary with other variables such as building, population, and road densities provides important insights into the processes that drive emissions patterns. Improved understanding of these processes is vital to designing effective emissions mitigation policies at urban and state scales.

At both local and regional scales, considerable progress has been made in validating the inventory estimates of emissions by comparing them with independent measurements of atmospheric CO_2 concentrations through the use of mesoscale chemical transport models (Brioude et al., 2013; Feng et al., 2016; Lauvaux et al., 2016). However, a major challenge in interpreting atmospheric CO_2 concentrations is that the daily and seasonal fluxes of carbon between the biosphere and atmosphere can be aliased with the similarly varying fossil fuel fluxes (Engelen et al., 2002; Geels et al., 2004; Hardiman et al., 2017; Hutyra et al., 2014; Shiga et al., 2014; Zhang et al., 2014). As fossil fuel fluxes are assumed to be more certain than the biosphere fluxes, particularly at continental scales, atmospheric inversion models designed to estimate net fluxes of carbon into or out of the biosphere have tended to assume low or zero uncertainty in the $FFCO_2$ flux (Ogle et al., 2015; Peters et al., 2007). However, this assumption of low uncertainties in $FFCO_2$ inventories is difficult to justify at subcontinental scales, as biases in spatial patterns of $FFCO_2$ fluxes can propagate through the transport model to bias posterior estimates of regional biogenic carbon sinks and sources. Several studies have demonstrated that errors in the characterization of $FFCO_2$ in continental-scale inversions can result in large (50%–100%) deviations in the retrieved estimates of biosphere carbon storage and fluxes (Gurney et al., 2005; Schuh et al., 2010).

In considering uncertainties in emissions inventories, it is necessary to distinguish between (1) uncertainty in the total emissions estimates (also referred to as "magnitude" uncertainty) and (2) uncertainty in the spatial and/or temporal distribution of emissions in the inventory domain (also referred to as "downscaling," "disaggregation" or "representation" uncertainty). It is challenging to directly estimate magnitude uncertainties for bottom-up inventories, as the underlying data are typically only available from a few sources, usually government agencies, and uncertainty estimates for these source data sets are rarely reported. Previous efforts to quantify magnitude uncertainties have relied extensively on "expert judgment" (Andres et al., 1996, 2014; Marland et al., 1985). These studies reviewed global and national data on fuel production and consumption, fuel energy and carbon content, and combustion/emission factors to select representative uncertainties in these terms for different categories of country. Marland et al. (1985) estimated global uncertainties of 6–10% in $FFCO_2$ emissions. Andres et al. (1996) used the magnitude of revisions to historical estimates of fuel consumption as a proxy for total uncertainty, estimating a mean global uncertainty of 8%.

At the national level, Gregg et al. (2008) used expert judgment and data on revisions to Chinese energy consumption to estimate uncertainties in U.S. emissions at 3–5% and Chinese emissions at 15–20%. Andres et al. (1996) grouped every country into one of seven groups based on perceived similarities in uncertainty. Andres et al. (2014) interpolated linearly between the Gregg et al. (2008) estimates for the U.S. and China and assigned uncertainty values along the interpolation to the seven country groups from Andres et al. (1996), with the resulting estimates of 2σ magnitude uncertainties thus ranging from 4 to 20% depending on the country.

Another common method used to approximate magnitude uncertainties has been to compare inventories of the same domain that are based on different data sources, as in Macknick (2014) and Hutchins et al. (2016). Although this approach does not explicitly account for the inherent uncertainties in each inventory, it provides an easily calculated estimate of the minimum uncertainty by considering the magnitude of disagreement across inventories. In these studies, energy statistics and/or emissions estimates were compared at national and global scales. Macknick (2014) estimated global uncertainty in fossil fuel consumption to be 9.2% in 2007, resulting in a 2.7% uncertainty in $FFCO_2$ emissions globally, but also found that national $FFCO_2$ emissions uncertainties exceeded 10% for seven of the largest emitters. Hutchins et al. (2016) compared U.S. emissions estimates from several of the most widely used global $FFCO_2$ inventory products, including the

Carbon Dioxide Information and Analysis Center (CDIAC) (Boden et al., 2017), Open-source Data Inventory for Anthropogenic CO_2 (ODIAC) (Oda & Maksyutov, 2011), Emissions Database for Global Atmospheric Research (EDGAR) (Olivier & Janssens-Maenhout, 2012), and Fossil Fuel Data Assimilation System (FFDAS) (Asefi-Najafabady et al., 2014), and found uncertainties of 8.7% at the national scale for the year 2008.

Efforts to estimate downscaling or representation uncertainties have focused on quantifying differences in the spatial patterns of emissions reported by different inventories and methods. This type of uncertainty exists because emissions estimates are almost always generated at a level of spatial aggregation that is coarser than the source activities that produce the actual emissions. These emissions estimates must then be downscaled to a grid format using spatial proxies that are believed to represent the patterns in source activity. While for some types of emissions this aggregation is relatively minimal (e.g., combining emissions from multiple smokestacks into a single "facility" location), for other sectors (e.g., road vehicles or buildings), emissions may be reported only at the state or county level. These coarser emissions must then be downscaled to the desired resolution, using data proxies that are available at that resolution (e.g., a map of the road network or population density). Imperfections in how these proxies accurately represent the "true" spatial pattern of emissions produces representation errors. Evaluating this type of uncertainty through inventory comparison was performed at the national level for the U.S. by Hutchins et al. (2016), who found that the spatial correlations between the major global inventories ranged from 0.35 to 0.98 depending on the grid resolution. Gately et al. (2015) found small differences in U.S. on-road CO_2 emissions at the national scale (~10%) but large differences at state and urban scales (50–100%).

Most of the widely used global $FFCO_2$ inventories utilize a downscaling approach, whereby national emissions totals are disaggregated using a variety of spatial proxies and statistical methods to assign national emissions totals to a grid. The Carbon Dioxide Information and Analysis Center (CDIAC) produces annual inventories at 1.0° resolution using population density as a spatial proxy to downscale national emissions estimates based on data from the United Nations Energy Statistics Yearbook (Boden et al., 2017; United Nations, 2014). ODIAC (Open-source Data Inventory for Anthropogenic CO_2) estimated monthly emissions at 1 km^2 using the same national totals as CDIAC but downscaled using a power plant database and a remotely sensed "nightlights" data product (Oda & Maksyutov, 2011). The Emissions Database for Global Atmospheric Research (EDGAR) estimated annual $FFCO_2$ emissions at 0.1° resolution using sector-specific spatial proxies to downscale national totals reported by the United Nations Framework Convention on Climate Change (Olivier & Janssens-Maenhout, 2012). The Fossil Fuel Data Assimilation System (FFDAS) estimated hourly emissions at 0.1° using a combination of a power plant database, satellite nightlights, and population density to downscale national emissions totals reported by the International Energy Agency (IEA) (Asefi-Najafabady et al., 2014).

National- or local-scale "bottom-up" inventories rely on considerably more detailed spatially and temporally resolved data to characterize the patterns of activities that generate $FFCO_2$ emissions. In the United States, the only currently available bottom-up $FFCO_2$ inventory with national coverage remains the Vulcan Project (Gurney et al., 2009), which estimated hourly $FFCO_2$ emissions from eight different source sectors at a 10 km^2 resolution across the continental U.S. for the year 2002. More recently, several other bottom-up inventories have been developed that focus on single source sectors (Gately et al., 2015, 2013; McDonald et al., 2014) or on local or regional emissions patterns (Feng et al., 2016; Gurney et al., 2012; Patarasuk et al., 2016). Comparisons of these new estimates with global inventories have revealed large differences in the magnitude and spatial distribution of emissions estimates, especially over large urban areas where the majority of emissions are believed to originate. For example, bottom-up studies have found that EDGAR overestimates urban vehicle emissions by 40–80% for cities in California (McDonald et al., 2014) and by as much as 100% for many of the largest U.S. cities while significantly underestimating emissions from the mostly rural interstate highway system (Gately et al., 2015, 2013).

In this study we present a new bottom-up estimate of $FFCO_2$ emissions at high resolution (hourly, 1 km^2), developed as part of a prototype carbon monitoring system (CMS) for the northeastern U.S. This new inventory, the Anthropogenic Carbon Emissions System (ACES), provides detailed, sector-specific estimates of carbon emissions at the spatial and temporal scales that are increasingly demanded by the mesoscale atmospheric and carbon cycle modeling communities, as well as both local and state-level policymakers. ACES is the first multistate regional inventory to report hourly $FFCO_2$ fluxes at a 1 × 1 km gridded

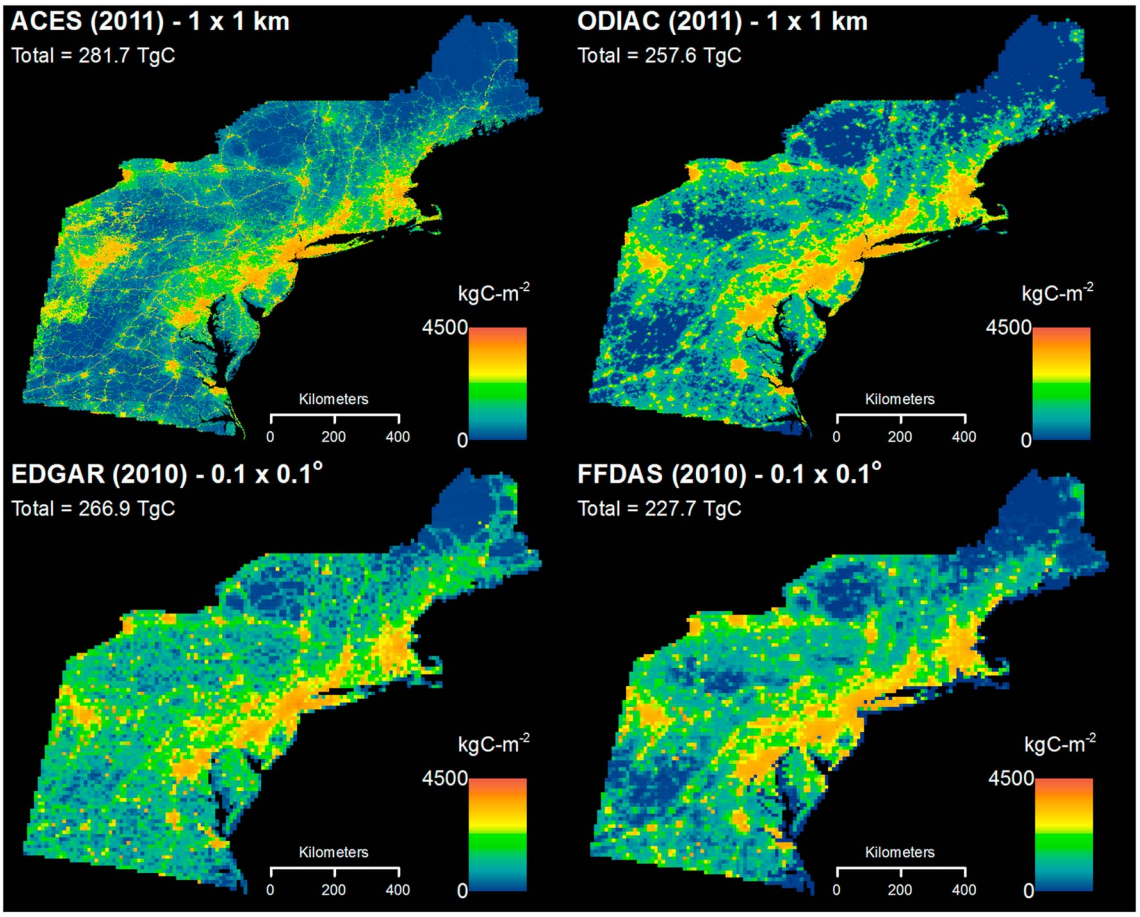

Figure 1. Anthropogenic carbon emissions from the northeastern U.S. from ACES, ODIAC, EDGAR, and FFDAS. ACES and ODIAC inventories are at their native spatial resolutions of 1 × 1 km. EDGAR and FFDAS are at their native resolution of 0.1° × 0.1°. ACES, ODIAC, and EDGAR are composed of $FFCO_2$ emissions from a nearly identical set of source sectors (ODIAC and EDGAR include emissions from airborne aircraft, ACES does not). FFDAS omits emissions from cement production, marine vessels, and aircraft.

resolution for all major carbon-emitting sectors, using an extensive database of high-resolution spatial proxies. We report magnitude uncertainties for the five largest source sectors in ACES (power plants, on-road, residential, commercial, and industrial) and combine those estimates to produce minimum total uncertainties in emissions across the whole ACES domain. We then characterize large downscaling uncertainties at regional and urban scales when ACES is compared with ODIAC, EDGAR, and FFDAS at multiple spatial resolutions. The impact of spatial aggregation on the emissions flux intensities of different source sectors and different inventories is evaluated, and we quantified the spatial correlations between the four inventories and between emissions and local population density. Finally, we quantified the urban area contributions to total $FFCO_2$ emissions at both the domain and state scales, revealing substantial variations in emissions source sector profiles between states.

2. Data and Methods

2.1. ACES—Anthropogenic Carbon Emissions System

We calculated annual and hourly CO_2 fluxes for nine different emissions sectors across the northeastern United States (Figure 1). ACES reports annual emissions for a base year of 2011 on a 1 × 1 km spatial grid, partitioned by emitting sector. The 2011 annual emissions were then used to calculate hourly emissions for two more recent calendar years, 2013 and 2014, holding the total emissions constant but accounting for seasonal and daily variations in meteorology, fuel consumption, and traffic patterns across these 2 years. A brief summary of the data sources and scaling methodology is presented here, with a detailed description

of all methods provided in the supporting information (SI). The full ACES data set is publically available for download at https://doi.org/10.3334/ORNLDAAC/1501.

Emissions of $FFCO_2$ from the residential, commercial, industrial, nonroad mobile, aircraft, marine, and rail sectors were derived from the U.S. Environmental Protection Agency's (EPA) National Emissions Inventory (NEI) for 2011 (United States Environmental Protection Agency, 2014a). Emissions from point sources, which include electric power generation, industrial facilities, and aircraft takeoff and landing operations, were estimated using a combination of data from the NEI and from the EPA Greenhouse Gas Reporting Program (GHGRP) (United States Environmental Protection Agency, 2014b). On-road CO_2 emissions were obtained from the Database of Road Transportation Emissions (DARTE) (Gately et al., 2015).

Aircraft sector emissions were estimated for near-surface emissions only, covering aircraft taxiing, takeoff and landing operations, and other ground-based airport vehicles and on-site stationary combustion sources. All emissions for this sector are treated as point sources located at the airport location reported by the NEI. Railway CO emissions were obtained from NEI and converted to CO_2 using emission factors from United States Environmental Protection Agency (2009a). Emissions were summed by county and then spatially distributed onto the NEI-provided "Rail Line Shape Files" GIS line shapefile. Marine vessel CO emissions from NEI were converted to CO_2 using emissions factors from United States Environmental Protection Agency (2009b) and assigned to waterways and port areas using the NEI "Port Area" shapefile. Additional details for these three sectors are provided in the SI. We do not calculate magnitude uncertainties for the aircraft, rail, and marine sectors, as the EPA does not report estimates of uncertainty for emissions, and there are no other available data sets with which to compare our ACES estimates. However, the combined emissions from these sectors comprise less than 1% of total $FFCO_2$ emissions in the ACES domain, so the overall impact of these unknown uncertainties on total emissions is expected to be very small.

For other point sources, NEI and GHGRP data were partitioned into electricity-generation facilities and non-electricity industrial facilities. For the 14,883 NEI point sources, CO emissions were converted into CO_2 emissions using emissions factors from United States Environmental Protection Agency (2014c) and from Gurney et al. (2010). The GHGRP reports emissions from each facility as CO_2, which reduces the uncertainty associated with conversion factors. Where possible we use the GHGRP emissions (N = 1,016). Annual, county-level CO emissions for nonpoint industrial sources were obtained from the NEI for industrial sources that are too small to be included in the NEI point source or GHGRP databases. For the GHGRP electricity-generating facilities, we calculated magnitude uncertainties following the methods described in Gurney et al. (2016). We compared annual $FFCO_2$ emissions reported by the GHGRP and the EPA eGRID database for 193 power plants in our ACES domain that were common to both databases. The mean relative difference between the GHGRP and eGRID estimates was 9.8%. We apply this mean uncertainty value to all power plants emissions (both NEI and GHGRP) in the ACES domain, resulting in a total uncertainty for this sector of ±8.8 Tg C (i.e., ±9.8% of the total sector emissions of 90.1 Tg C).

For the DARTE on-road emissions, we calculated magnitude uncertainties following the methods used in Gately et al. (2013) and Mendoza et al. (2013). We used 1 sigma uncertainties in the levels of vehicle miles traveled reported by the Federal Highway Administration (2017) and then propagated these uncertainties through the DARTE emissions model. See Gately et al. (2013) for details of this procedure. Total uncertainty for this sector was ±5.8 Tg C (i.e., ±7.1% of the total emissions of 81.7 Tg C). Annual CO_2 emissions were then downscaled to hourly estimates using hourly vehicle counts obtained from 492 in-road automatic traffic recorders spread across the domain (Figure S6). See the SI for more details.

For emissions from vehicles operating off of the public road network (e.g., construction vehicles, agricultural vehicles, and lawn equipment), estimates of county-level CO_2 were obtained from the NONROAD2008 model included in the EPA MOVES2014a (Motor Vehicle Emission Simulator) model, available at http://www.epa.gov/otaq/nonrdmdl.htm. Nonroad emissions were given a uniform spatial distribution within each county, as no data on within county spatial patterns were available. Due to data paucity, no uncertainty estimates were made for this sector.

For the residential, commercial, and nonpoint industrial sectors we use NEI reported emissions of CO at the county scale. We convert CO to CO_2 using emissions factors from the EPA WEBFire database (United States Environmental Protection Agency, 2014c) and from Gurney et al. (2010) depending on fuel type and

combustion process (Appendix A in the SI). For these three sectors, the NEI estimates rely on a combination of state and county level data on fuel consumption reported by both the states themselves and by the Energy Information Administration's State Energy Data System (SEDS). As none of these sources of data report uncertainties for their emissions or fuel consumption estimates, a direct calculation of magnitude uncertainty for these sectors is not possible. We approximate an estimate for this uncertainty by comparing our ACES state total CO_2 emissions to the SEDS sector total estimates for the states that are wholly contained within our domain. We aggregated the commercial and industrial emissions from both data products for this comparison, so as to avoid potential issues arising from differences in how emissions are assigned between these categories. We calculated the differences in emissions estimates for each state, summed these over all states, and then divided by the mean of the total SEDS and total ACES emissions for those states. This produces a "percent relative difference" (RD) statistic that approximates the magnitude uncertainty in total emissions for each of these sectors across the whole domain. For the residential sector the RD was 12.8%, and for the industrial/commercial sector the RD was 7.8%. Magnitude uncertainties for each ACES sector as a whole were calculated as the total sector emissions plus/minus the total emissions multiplied by the sector RD. We also calculated RD values for the electric power sector using the above methods and found the RD for that sector to be only 3.3%. As this was smaller than the uncertainty estimate of 9.8% calculated using the eGRID versus GHGRP method described above, we retained that larger value of uncertainty for that sector in our results.

Commercial emissions were downscaled from county to Census Block using the number of jobs in each block obtained from the Longitudinal Employment-Household Dynamics database (LODES) (United States Census Bureau, Center for Economic Studies, 2014). LODES was not available for Massachusetts; therefore, the Massachusetts Tax Assessor Parcel data (Metropolitan Area Planning Council, 2014) were used to assign emissions based on the building square footage within each commercial-use parcel. For the LODES data, the number of jobs in each Census Block was divided by the total jobs in the county to produce an allocation factor. For the Massachusetts parcel data, the square footage of each parcel was divided by the total square footage in the county to produce the allocation factor. County total emissions were then multiplied by the factor for each block (parcel) to produce block (parcel) total emissions estimates. For residential sector emissions, we use a similar method to downscale from the county totals to Census Block Groups, using data on the number of households in each Census Block Group partitioned by type of home heating fuel (United States Census Bureau, 2015). See the supporting information for more details.

CO_2 emissions associated with oil and gas production at the county level were calculated using the EPA Oil and Gas Emission Estimation tool (http://www.epa.gov/ttnchie1/net/2011inventory.html). Data on oil and gas wellhead locations were obtained from multiple state sources (New York State Department of Environmental Conservation, 2016; Pennsylvania Department of Environmental Protection, 2016; Virginia Department of Mines, Minerals, and Energy, 2016; West Virginia Department of Environmental Protection, 2016) and used to assign emissions to individual wellheads within each county. Due to data paucity, no uncertainty estimates were made for this sector. Emissions from this sector comprise 3.5% of total ACES emissions in the domain; the impact of these unknown uncertainties is expected to be small.

2.2. Inventory Comparisons and Statistical Analysis

To quantify uncertainties in the spatial distribution of $FFCO_2$ emissions, we compared our ACES inventory to the three most widely used gridded inventories: ODIAC, EDGAR, and FFDAS. ODIAC is available for 2011 at 0.083° (~1 km^2) resolution, while EDGAR and FFDAS are both available for the year 2010 at 0.1° resolution. From 2010 to 2011 U.S. emissions changed by only −2.3%, so the interannual difference between inventories should be relatively small for the northeast domain. A common challenge in comparing $FFCO_2$ inventories is variable source sectors included by different inventories, as well as the definitions of these sectors, as they are often inconsistent across inventories. In this case, EDGAR and ODIAC both comprise all of the same sectors as our inventory, with the exception that both include airborne aircraft emissions, whereas ACES includes only aircraft takeoff and landing emissions. FFDAS does not include emissions from oil and gas production, air and marine transport, or cement manufacturing, although for our study domain these differing sectors represent only 4.3% of total $FFCO_2$ emissions (12.2 Tg C) as estimated by ACES, so the comparison of all four inventories is relatively consistent. We compare all inventories using their reported total $FFCO_2$ emissions, with no efforts made to harmonize sectors or years. Differences in inventory emissions will therefore reflect all sources of deviation, including the slight mismatches in vintage and sectoral composition. We also compare the ACES

inventory with the Vulcan inventory (Gurney et al., 2009), which reports emissions from the year 2002. Although Vulcan is the only other available bottom-up inventory for the U.S., its vintage year of 2002 limits its utility for comparison with the 2011 ACES. To isolate the differences associated with the spatial distribution of emissions between the two products, we scaled the total Vulcan emissions to match the ACES totals and calculated pixel scale differences (Figure S8 and related text in the supporting information).

To evaluate the spatial uncertainty across the four contemporaneous inventories of ACES, ODIAC, EDGAR, and FFDAS, we calculated the percent RD between all inventories at the grid cell scale. We define RD here as the difference between the highest and lowest emissions estimate in each grid cell divided by the mean of all inventories' emissions estimates for that grid cell. Note that this is slightly different from how RD is defined in Andres et al. (2012). The RD statistic provides a conservative estimate of the uncertainty in emissions at local scales as the use of the unweighted mean of the four inventories implicitly assumes that for a given grid cell the emissions estimate from each inventory is equally plausible. We observe that FFDAS and ODIAC report zero values for emissions in many locations where emissions-generating source activities are known to be present. In these cases, the calculated RD overestimates the uncertainty, as the zeroes would otherwise be dropped given this outside knowledge. Finally, we calculated the Pearson correlation coefficients (r) between all pairs of inventories and between each inventory's emissions and population (obtained from the LandScan population database (Oak Ridge National Laboratory, 2014)) at both the inventory's native spatial resolution and a series of coarser resolutions.

3. Results

3.1. ACES—Anthropogenic Carbon Emissions System

We estimate a total annual fossil fuel carbon flux of 281.7 ± 24.3 Tg C (445.8 ± 38.5 Mg C km^{-2}) across our 631,811 km^2 study domain (Figure 1). The sector-specific uncertainty calculations described in section 2.1 were summed linearly to produce the overall magnitude uncertainties reported here. Within the northeast U.S. domain, emissions from on-road transportation contributed 29% (81.7 ± 5.8 Tg C), electric power generation contributed 32% (90.1 ± 8.8 Tg C), industrial and commercial sources contributed 21.8% (63.3 ± 4.9 Tg C), and residential energy consumption contributed 12.8% (37.1 ± 4.8 Tg C). Due to data limitations, it was not possible to calculate uncertainties for all sectors contained in ACES; however, the reported uncertainties comprise >95% of emissions in the domain. In relative terms, the overall uncertainty in total ACES emissions across the domain is ±8.6%.

We evaluated the share of emissions in each state of our domain that occurs within "urban" areas based on the U.S. Census urbanized areas and urban clusters (UAs) boundaries (Figure 2). The urban shares of state emissions are highly variable, ranging from 25 to 85% of total state emissions (100% when including the District of Columbia), with a domain-wide urban emissions share of 57%. Across the 13 states in the domain, residential and commercial buildings and the on-road sector consistently dominate urban emissions, but the relative proportions vary considerably. Electric power generation is not typically a large urban emission source as these facilities are often outside city centers (Providence, RI, being a notable exception). Within urban areas we also observe significant differences in the dominant diurnal patterns of emissions (Figure S2). For example, in NYC during the winter, downtown Manhattan has a diurnal emissions pattern dominated by meteorology-driven building heating demand, whereas in parts of the outer boroughs such as Queens daily emissions patterns are dominated by on-road sector emissions, which follow a recognizable morning and evening bimodal peak (Figure S2).

3.2. Inventory Comparison

At the domain scale, we find that ACES and EDGAR estimates are the most similar, with EDGAR reporting 266.9 Tg C, only 5% less than ACES in aggregate. ODIAC is the next closest at 257.6 Tg C, 10% less than ACES. FFDAS reports the lowest emissions for the domain, 227.7 Tg C, more than 20% less than ACES, although some of this difference is likely due to FFDAS' exclusion of some emitting sectors (in ACES those sectors comprise ~4.3% of total emissions). Since each of the non-ACES inventories is based on national total emissions estimates, the regional differences are also likely to be a result of differences in the regional shares of the different spatial proxies used by each inventory to downscale these national totals. Despite the larger differences in total emissions of ACES, ODIAC, and FFDAS, at subregional scales those inventories' spatial

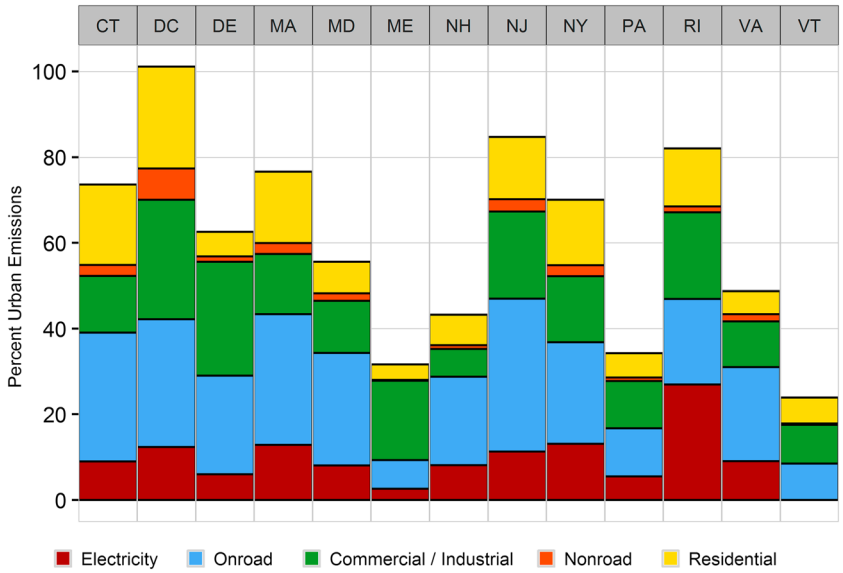

Figure 2. Share of $FFCO_2$ emissions in each state that occur in census urbanized areas (UAs). For the whole domain, 57% of emissions occur in UAs. At the state level, urban emission shares vary considerably, with the on-road and commercial/industrial sectors showing the most variation in their relative shares of urban emissions.

patterns of emissions are more consistent than those of EDGAR (Figure 1). ODIAC and FFDAS show similar spatial patterns, reflecting their common use of nightlights and power plant data sources (Oda & Maksyutov, 2011; Asefi-Najafabady et al., 2014). However, EDGAR allocates a significant share of emissions into the central cores of the region's largest urban areas and also allocates higher emissions in rural areas than the three other inventories (Figure 1). Most notably, EDGAR appears to distribute on-road emissions much more homogenously across the domain than ACES or the other downscaled inventories. The domain-wide coefficient of variation (CV) of emissions intensity for EDGAR line source emissions (on road + railway) shows small declines with aggregation, from 0.93 at 10 km^2 down to only 0.8 at 40 km^2 (Table 1). By contrast, the CV of ACES line source emissions declines significantly with aggregation, from 6.6 at 1 km^2 to 2.71 at 10 km^2 and then down to 1.99 at 40 km^2. The insensitivity of EDGAR line source emissions intensity to spatial aggregation implies a relative lack of spatial variability in that EDGAR sector.

To compare all of the inventories at a consistent resolution, we aggregated ACES and ODIAC up to a 0.1° grid to match the native resolutions of EDGAR and FFDAS. Figure 3 shows the absolute and relative grid cell-scale differences between all four inventories for the domain. At 0.1° resolution, the mean grid cell RD is 120%. We observe large values of RD (>100%) for almost half of all grid cells in the domain, and over 75% of all grid cells have RDs >50%. The areas with the largest absolute differences are concentrated in the urban cores of the major cities, along much of the Atlantic coast, and in the oil and gas intensive regions of western PA and

Table 1
Domain-Wide Coefficients of Variation (CV) for ACES and EDGAR by Sector Class

	ACES				EDGAR			
Resolution	All sectors	Point	Line	Area	All sectors	Point	Line	Area
1 km^2	34.72	81.61	6.60	5.44	-	-	-	-
5 km^2	7.65	16.90	3.37	3.99	-	-	-	-
10 km^2	4.38	8.83	2.71	3.44	3.73	6.54	0.93	4.78
20 km^2	2.70	4.57	2.30	2.85	2.83	4.35	0.87	4.32
40 km^2	2.05	2.76	1.99	2.65	2.28	2.82	0.80	3.76

Note. Aggregation from 1 km^2 to coarser resolution grid scales reduces spatial variation in emissions at the domain scale, lowering the CV. For ACES, the spatial variability of point source and line source emissions is the most sensitive to aggregation, due to their inherently higher spatial heterogeneity. For EDGAR, line source emissions are notably homogenous in their spatial distribution, with little changes to their CV even when scaled to 40 km^2 grid resolution.

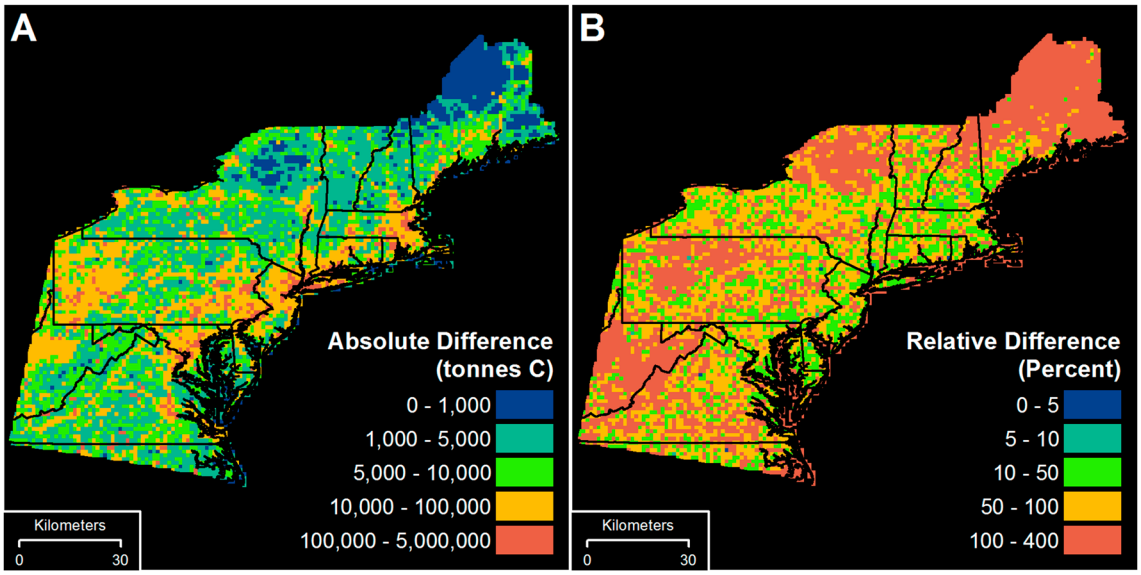

Figure 3. Uncertainty between regional-scale $FFCO_2$ inventories at 0.1° resolution. (a) The absolute difference between the highest and lowest emissions reported in each grid cell. (b) The relative difference (RD) in percent (absolute difference divided by mean emissions of each grid cell). Absolute differences are largest in urban areas and in the oil and gas production regions of western Pennsylvania and West Virginia. Large RDs are also observed across most of the domain, with urban areas and the oil and gas sector dominated regions also standing out. The large RD values observed in northern Maine, New York, and central Pennsylvania reflect areas where the non-ACES inventories report zero emissions but ACES reports small but nonzero emissions.

WV. The highly visible discrepancies in $FFCO_2$ emissions in western PA and WV reflect the fact that none of the three downscaled inventories are designed to capture the emission signature from the recent expansion of oil and gas development across that region. For the state of PA, oil and gas sector emissions account for almost 9% of state total emissions in ACES, with nearly all of those emissions occurring in the western third of the state. Identifying the magnitude and spatial location of these emissions is vital to support regional mitigation efforts.

The urban areas with large discrepancies between inventories are also the areas with the highest overall emissions, which is even more critical from a mitigation policy perspective. For the urban area grid cells (based on the census UAs), the mean RD is 84%. For over one quarter of these urban grid cells the RDs range from 100% to as high as 300%. The highest RD values are found in the grid cells in the largest urban areas in the domain, which are again the areas with the largest concentrations of total emissions.

For the largest urban area in our domain, New York City, NY (NYC), we calculated the pixel-scale RD in emissions across (1) all four inventories, (2) across only the downscaled inventories (ACES excluded), and (3) for just the two high-resolution inventories (ACES and ODIAC) (Figures 4 and S4). The mean RD of NYC grid cells, when all inventories are considered, is 92%. When ACES is excluded, the mean RD falls to 76%. The better agreement when ACES is excluded is due to the inherent similarities of ODIAC and FFDAS, which use the same source data and similar spatial scaling algorithms. At 1 km^2 resolution, the RDs between ACES and ODIAC are also large (Figure S4c), with a mean RD of 71% and an RD $>$ 100% for over half of the grid cells.

Evaluating the three downscaled inventories relative to ACES, we find that FFDAS underestimates by 50% or more across much of the core urban area (Figure S5a), while EDGAR overestimates, relative to ACES, by 75% or more in both the urban core and in the surrounding suburbs (Figure S5b). When compared with ACES at 1 km^2 resolution, ODIAC shows the largest observed differences in grid cells dominated by on-road emissions (Figure S5c), as it underpredicts ACES by $>$75% in most of the grid cells containing major roads. At 10 km^2 resolution (Figure S5d), there is considerable improvement in spatial agreement between ACES and ODIAC, with the mean RD falling to 44.8%, and only one third of grid cells having RDs $>$50%.

3.3. Scale Sensitivity

Aggregating emissions to a coarser spatial grid tends to "smooth out" local gradients in emissions, as concentrated point and line sources are spatially averaged with lower intensity areal sources. To measure the impact

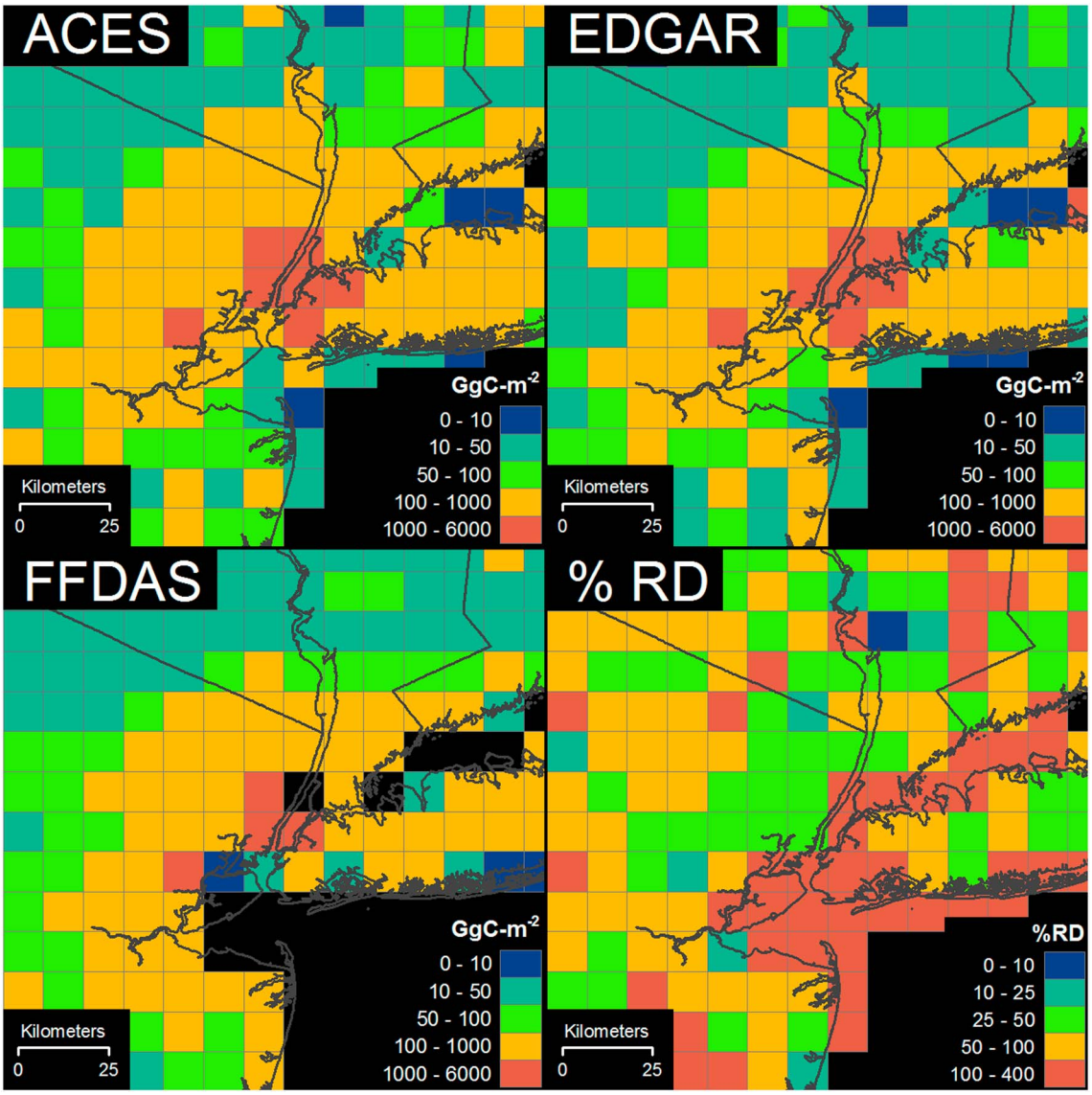

Figure 4. Comparison of emissions inventories for the New York City, NY, metropolitan area at 0.1° scales (ODIAC not shown). Many of the coastal grid cells in FFDAS contain values of zero emissions, most notably in upper Manhattan. EDGAR concentrates emissions in the core of the city, while ACES and FFDAS are higher in the suburban areas. The bottom right panel shows percent relative difference (RD) between all inventories (ODIAC included). The mean RD for the area shown is 83%, with much of the core urban area showing RDs of greater than 100%.

of spatial aggregation on $FFCO_2$ gradients in our domain, we aggregated the ACES, ODIAC, EDGAR, and FFDAS inventories to 5 km^2, 10 km^2, 20 km^2, and 40 km^2 resolutions. At each resolution we calculated the within cell CV of emissions with respect to the distribution of the 1 km^2 grid cell emissions (equation (S1)). This within pixel CV provides a normalized estimate of the localized reduction in the spatial variation of emissions that occurs when emissions are averaged to a coarser resolution. In general, grid cells with a larger CV represent areas where spatial aggregation has "smoothed out" large gradients in local emissions, for example, power plants surrounded by low-emissions rural areas, or large freeways passing through low-density suburban towns.

For ACES and EDGAR we calculated CVs for total emissions and for two sectors: residential and on-road emissions (Figures 5a–5c). For ACES, the distribution of grid cell CVs becomes increasingly right skewed and platykurtic with aggregation, with the mean CV increasing from 1.7 at 10 km^2 to 8.1 at 40 km^2. This "widening" of the distribution is most pronounced for total $FFCO_2$ emissions; for the residential sector, the mean CV increases from 0.8 to 2.6, and for the on-road sector from 2.0 to 3.8 (Figures 5b and 5c). For EDGAR we

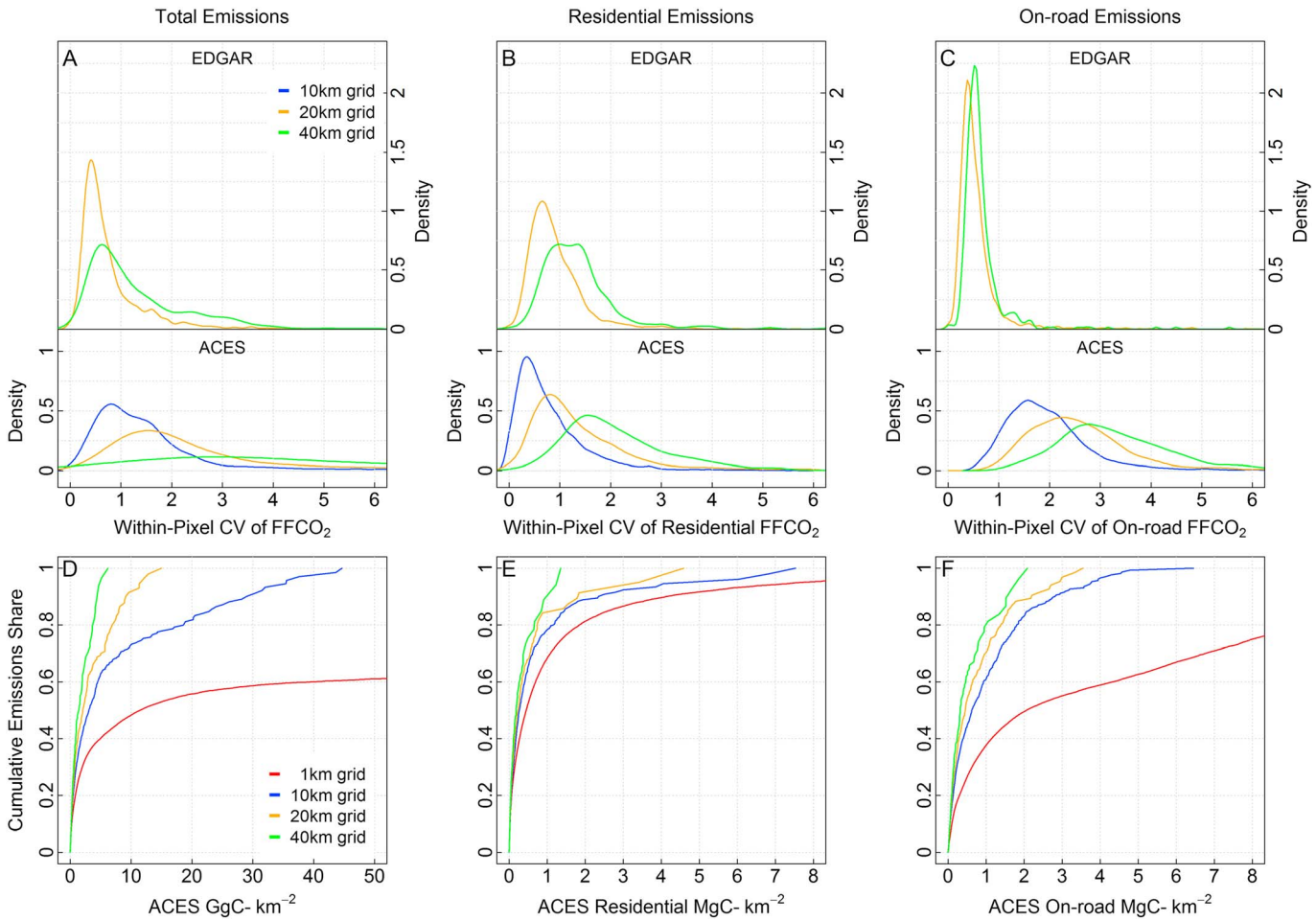

Figure 5. Distribution of within grid cell coefficient of variation (CV) of $FFCO_2$ for different grid resolutions. CV values reflect the within cell variation in emissions that is smoothed out by spatial aggregation. (a) For ACES total emissions, the mean CV increases from 1.7 to 8.1 going from 10 km^2 to 40 km^2 resolutions. The increase in mean CV with aggregation is less for the (b) residential sector (0.8 to 2.6) than for the (c) on-road sector (2.0 to 3.8). For EDGAR, the CV distribution is less affected by aggregation below 40 km^2, with the on-road sector in particular showing almost no change in mean CV (0.45 to 0.69, Figure 5c). (d–f) Changes in the cumulative distributions of ACES grid cell emissions intensity due to spatial aggregation. The CDF of ACES residential emissions is least affected by aggregation (Figure 5e), compared to total emissions (Figure 5d) and on-road emissions (Figure 5f).

found a significantly smaller change in the grid cell CVs, with mean CV increasing from 0.5 to 1.3. As with ACES, we found that EDGAR total emissions and residential sector emissions also become more right skewed and platykurtic as grid cell size increases. EDGAR on-road CVs (Figure 5c) are tightly distributed with a long, fat right tail, and a mean and standard deviation of only 1.4 and 0.7, respectively, at 40 km^2. This pattern suggests that the scaling factor used to distribute EDGAR on-road emissions is very scale invariant, that is, highly uniform. This is in sharp contrast to the ACES on-road emissions, which are spatially assigned to a national road network that shows considerable spatial variation in areal density (Gately et al., 2015).

Analysis of the cumulative share of total emissions versus grid cell emissions intensity ($FFCO_2$ per square kilometer) for ACES (Figures 5d–5f) show that the residential sector is least sensitive to aggregation, while for on-road and total emissions, aggregation to 10 km^2 or coarser significantly shifts the cumulative distribution of emissions. In general, aggregation to coarser grid cell size tends to reduce areal emissions intensity, as large emissions sources with small spatial extents, such as roads and power plants, are combined with lower intensity area sources, such as buildings. This effect is visible in all of the cumulative distribution plots shown in Figures 5d–5f. This shift is clearly visible for the ACES total emissions (Figure 5d), as the maximum emissions intensity declines by almost 2 orders of magnitude from 4,415 Gg C km^{-2} at 1 km^2 resolution to only 44.6 Gg C km^{-2} at 10 km^2 resolution. At 10 km^2, ACES grid cells with total emissions intensities of

Table 2
Pearson Correlations (r) Between ACES and Other Inventories as a Function of Grid Spatial Resolution

Grid	ODIAC	EDGAR	FFDAS	EDGAR point	FFDAS point	EDGAR area	FFDAS area	EDGAR line
1 km	0.50	-	-	-	-	-	-	-
5 km	0.84	-	-	-	-	-	-	-
10 km	0.87	0.66	0.69	0.53	0.60	0.90	0.72	0.77
20 km	0.90	0.84	0.84	0.71	0.75	0.94	0.77	0.84
40 km	0.95	0.93	0.93	0.85	0.85	0.94	0.85	0.87

Note. ODIAC exhibits the best correlation with ACES at all resolutions. Correlations are generally low for EDGAR and FFDAS at 10 km^2 but improve at coarser resolutions. Line and area source emissions have higher correlations at high resolution ($r > 0.7$ at 10 km^2), but point source emissions only correlate well at 20 km^2 and above.

5 Gg C km^{-2} or less comprise over 60% of total emissions, while at 1 km^2 only 40% of emissions come from grid cells emitting 5 Gg C km^{-2} or less, and 40% of emissions come from grid cells with emissions intensity larger than 44 Gg C km^{-2}. All of these higher-intensity emissions fluxes are smoothed out by aggregation from 1 km^2 to 10 km^2. At coarser resolutions emissions intensities are even further reduced, with over 90% of emissions at 20 km^2 originating from cells at 10 Gg C km^{-2} or less (Figure 5d). On-road emissions show a similar shift in the distribution of emissions intensities going from 1 km^2 to 10 km^2, but further aggregation does not shift the cumulative emissions distribution as drastically as with total emissions, with similarly shaped distributions at 20 km^2 and 40 km^2 resolutions (Figure 5f). Residential emissions are the least affected by aggregation, with emissions intensities staying consistent for grid cells comprising over 80% of emissions at all scales (Figure 5e). These results are consistent with the inherent spatial distribution of these sectors: roads are both more spatially compact and more heterogeneously distributed across the landscape than residential buildings, and thus, decreasing grid resolution tends to, on average, incorporate more "nonroad" areas than "nonresidential" areas into a grid cell.

Overall, spatial aggregation reduces the domain-wide CVs of emissions while improving the spatial correlations between the different inventories and between inventory emissions and population (Tables 1–3). For ACES, the domain-wide CV of total emissions decreases by nearly an order of magnitude between 1 km^2 and 10 km^2 resolutions, from 34.7 to 4.4. Point source and line source emissions exhibit the largest change in spatial variability with aggregation, due to their inherent spatial heterogeneity. For EDGAR both the absolute and relative decreases in total emissions CV are much smaller, from 5.0 to 2.3. EDGAR point source emissions also show large reductions in CV with aggregation, but EDGAR on-road emissions exhibit notably low spatial variability, even at fine resolutions. At 10 km^2 and up, EDGAR point and area source emissions have similar CVs to ACES.

To evaluate the overall correlation between each inventory and ACES, we calculated domain-wide spatial correlations for multiple grid resolutions (Table 2). ODIAC shows the best correlation with ACES at all spatial scales. Correlations with EDGAR and FFDAS are relatively low at 10 km^2, although when only area source emissions are considered correlations improve.

Population density is often used as a spatial proxy for emissions (Andres et al., 2014; Asefi-Najafabady et al., 2014; Olivier & Janssens-Maenhout, 2012), although it has been shown that the relationship between emissions and population is not spatially homogenous (Hogue et al., 2016), and for sectors like on-road emissions is nonlinear at regional and local scales (Gately et al., 2015). Since none of the emissions estimates in ACES use population as a spatial proxy, we were able to compare emissions to an independent measure of population density (Oak Ridge National Laboratory, 2014) at multiple spatial scales (Table 3). We also compute correlations with population for the other inventories. For the whole domain at 1 km^2, the Pearson correlation between ACES total emissions and population is only 0.06. Examining individual source sectors by their inherent spatial patterns (point, line, and area sources) for ACES, EDGAR, and FFDAS, we observe that area sources have the strongest correlations with population (0.96, 0.93, and 0.74, respectively, at 10 km^2 resolution). At resolutions below 10 km^2 ACES line source emissions have low correlations with population, while point source emissions are poorly correlated at all spatial scales for all inventories ($r < 0.37$ at 40 km^2). The low correlations of point and line sources with population at higher spatial resolutions likely contribute significantly to the large discrepancies observed between ACES and the downscaled inventories.

Table 3
Pearson Correlation (r) Between Each Inventory's $FFCO_2$ Emissions and the Average Daytime Population Reported by the LandScan Population Database (Oak Ridge National Laboratory, 2014)

Grid (km)	ACES	ODIAC	EDGAR	FFDAS	ACES point	EDGAR point	FFDAS point	ACES area	EDGAR area	FFDAS area	ACES line	EDGAR line
1	0.06	0.04	-	-	0.01	-	-	0.90	-	-	0.24	-
5	0.27	0.20	-	-	0.09	-	-	0.96	-	-	0.55	-
10	0.50	0.36	0.66	0.47	0.19	0.30	0.20	0.96	0.93	0.74	0.71	0.63
20	0.68	0.53	0.76	0.56	0.27	0.33	0.23	0.97	0.97	0.78	0.81	0.67
40	0.77	0.66	0.80	0.69	0.36	0.37	0.27	0.95	0.98	0.87	0.89	0.74

Note. Overall correlations are low for total emissions at resolutions below 20 km^2. Area source emissions show the best correlations with population, with ACES showing the strongest correlation at finer spatial resolutions. Line source emissions show only moderate correlations below 20 km^2 resolution.

4. Discussion

Our comparison of ACES with three of the most commonly used global $FFCO_2$ inventories shows that even at broad regional scales the overall uncertainty in emissions estimates is as high as 20% (Figure 1). While the ACES inventory itself has a relatively modest total uncertainty of ~8.6%, the overall disagreement between ACES and the major global inventories implies that this uncertainty may be somewhat larger. Two inventories constructed from the same data sources (i.e., ODIAC and FFDAS) report different regional emissions totals (Δ12%) for our domain, emphasizing how minor differences in included source sectors and the downscaling algorithms can produce significant differences at subnational scales. These results add additional support to the growing consensus that the overall uncertainties in $FFCO_2$ inventories are larger than were initially thought (Andres et al., 2014; Ciais et al., 2014; Gately et al., 2015; Miller & Michalak, 2016; Oda et al., 2015).

The magnitude of these uncertainties threatens to undermine the confidence of state and local policymakers to accurately monitor and detect trends in emissions, especially at urban scales. Without this confidence in the accuracy of inventories, it is then difficult to assess the performance of any mitigation policies that are implemented, which reduces accountability and can prevent the objective evaluation of whether declared climate action targets are being met. Even in countries with highly developed energy statistics and data infrastructure, the data that underpin emissions estimates are typically published by just a few government sources, with no reported estimates of potential errors. Nonetheless, these data are often taken at face value, as they are considered the most accurate estimates of the total amounts of fossil fuels burned, and by proxy, the total amounts of CO_2 released from their combustion. However, recent research has suggested that sector-specific and subnational uncertainties are considerably higher than previously believed. Gurney et al. (2016) found significant differences in the total annual CO_2 emissions reported for the same power plants by two different U.S. agencies (monthly differences $>$13% for one fifth of U.S. power plants). We confirm that result in this study, finding mean differences of almost 10% between eGRID and GHGRP power plant emissions within our ACES domain. Hogue et al. (2016) found that for large parts of the eastern U.S., the spatial uncertainty of point source locations produces uncertainties as high as 25% of the total emissions in each 1° grid cell. Hogue et al. (2016) also showed that downscaling national emissions to 1° grid cells using a single national value for per capita emissions produced mean absolute biases of 150% compared to emissions downscaled using state-level per capita emissions values.

At local scales, the downscaled inventories vary widely in their estimates, as well as deviating significantly from our bottom-up inventory. For the NYC metropolitan area, the mean total emissions of the four inventories is 34.3 Tg C, but the range of estimates varies from 26.5 Tg C (FFDAS) to 41.4 Tg C (EDGAR), a representation uncertainty of almost 28 Tg C, equivalent to 80% of the metropolitan area's mean emissions. ACES and ODIAC emissions are near the mean, (38.2 Tg C and 31.1 Tg C, respectively) but also show the largest pixel-level differences when the two inventories are compared directly at their native 1 km^2 resolution. These deviations appear to reflect the spatial patterns in source activity that are well represented in ACES, particularly line source emissions from major roads, but that are not captured by the population- and nightlights-based downscaling in ODIAC. While ODIAC and the other global inventories were not designed to be used for this type of urban analysis, they have been applied to a wide range of urban- and regional-scale modeling and policy analyses (e.g., Brioude et al., 2013; Hakkarainen et al., 2016; Marcotullio et al., 2012; Sarzynski, 2012; Schneising et al., 2013; Shiga et al., 2014; Tohjima et al., 2014; Turnbull et al., 2011; Vogel et al., 2012; Wunch et al., 2009; Yadav et al., 2016). Indeed, the high-resolution grids of these inventories (1–10 km) appear to

imply a fidelity at these local scales that is not necessarily evident. The large uncertainties we report here serve as a strong caution to future researchers that these inventories do not appear to provide accurate representations of $FFCO_2$ emissions at subnational or urban scales.

Like many cities worldwide, New York City has committed to ambitious emissions reductions targets: 80% below 2005 levels by 2050, with a 40% reduction by 2030 and a 30% reduction in building emissions by 2025 (City of New York, 2015). Bottom-up inventories performed by the city estimated emissions equivalent to 14.8 Tg C in 2010 and 14.6 Tg C in 2011 (City of New York, 2011; City of New York, 2012). When we sum emissions for 2011 from ACES and the other inventories using only the grid cells covering New York City proper, ACES reports 13.6 Tg C and ODIAC reports 8.6 Tg C. For the year 2010, EDGAR reports 15.8 Tg C, while FFDAS reports 5.9 Tg C. The largest deviations from the local NYC inventory, ODIAC (−41%) and FFDAS (−60%), are the two inventories that use only power plants, population, and nightlights as spatial proxies. ACES and EDGAR both estimate emissions to within 1 Tg C of the totals reported by the NYC inventory, equivalent to roughly a ± 7% mismatch. While ±7% is still a significant difference, it is considerably smaller than the targeted reductions in NYC's climate action plan (40%–80%) and is on par with the overall margin of error estimated for ACES (8.6%). The single-year discrepancies of >40% observed with the ODIAC and FFDAS inventories are comparable in magnitude to the emissions reduction targets that NYC has established for the next 20–40 years (City of New York, 2015). Accurately monitoring emissions reductions on shorter time scales (i.e., annually) requires a significantly lower level of representation uncertainty in the inventory estimates than is provided by the downscaled global products, compared to the bottom-up methods used by ACES and by the City of New York's in-house inventory. We further evaluate the performance of ACES and the other inventories against independent bottom-up estimates by comparing them with locally produced inventories published by 11 other cities across the region (Figure S7). We find that the ACES estimates are most similar to the city-reported values (mean RD of 33%, compared to 57%, 65%, and 78% for ODIAC, EDGAR, and FFDAS, respectively), confirming that ACES provides more accurate representations of $FFCO_2$ emissions at urban scales than the downscaled global inventories.

Beyond NYC, other urban-scale efforts to reduce emissions of CO_2 from anthropogenic sources will have a similar need for locally derived estimates of emissions, but not all of these cities and municipalities will have the resources necessary to develop their own custom bottom-up inventories based on local data. ACES can provide a valuable benchmark of emissions for these small- and medium-size cities, and its regionally consistent methodology allows for the direct comparison of emissions across all cities and urban areas in the domain.

Policymakers at all levels of government continue to strive to understand the underlying drivers of emissions from different type of human activities, so as to design efficient policies that target specific aspects of economic, administrative, or technologic processes. For example, increasing the density of urban populations through residential and commercial development and urban planning is widely seen as a positive effort toward reducing per capita emissions in large cities (Jones & Kammen, 2014; National Research Council, 2009). However, in order to evaluate the emissions impacts of these sorts of policies at urban scales, it is necessary to use estimates of emissions that do not rely on population for their spatial distribution. Although at coarser scales population is a good predictor of emissions, we have shown here that this relationship is not sustained at urban scales. In particular, our results suggest that it is largely the low correlation of population with point and line source emissions (Table 3) that drives the uncertainty between inventories at local scales. This uncertainty is most pronounced for the large urban areas, where the low correlations with point and line source emissions may explain the significant spatial mismatches observed between the ACES bottom-up inventory and the population-downscaled global inventories (FFDAS and EDGAR) in cities such as NYC. Inventories like ACES that are constructed for the most part independently from local population data will allow policymakers and researchers to directly examine the functional relationships between emissions and spatial covariates, such as population density, so as to develop effective urban planning policies to reduce future emissions.

A U.N. report on global trends in urbanization (United Nations, 2012) finds that urban areas are responsible for as much as 70% of global $FFCO_2$ emissions. Although this is a very widely cited statistic, the report, in fact, estimates that direct emissions from urban areas (emissions actually occurring within the areas classified as urban as opposed to external emissions associated with power generation or imported goods consumed

within urban areas) actually comprise only 40% of emissions globally. The report also notes that the uncertainty in these estimates is potentially very large, as there exists no common standard for classifying land as urban, and even for calculations of "direct" emissions different $FFCO_2$ inventories will vary in what is included in terms of source sectors. Looking across the 13 states in our northeastern U.S. domain, variations in urban populations, urban extent, and dominant economic and industrial activities results in very different state-level emissions profiles. Although 57% of emissions in the domain occur in Census Urbanized Areas, five states have less than half of their emissions occurring in urban areas, while six others contain more than 75% urban emissions (Figure 2). For all states, the on-road sector dominates emissions at both urban and state levels, but the relative contributions of industrial activity and electric power generation vary widely across the region. Vermont for example has almost zero emissions from electric power and less than 7% from industrial activities (Figure S3). In contrast, over 60% of Pennsylvania's emissions come from power generation and industrial activity, with oil and gas production alone accounting for 9% of the state's total CO_2 emissions. The most urbanized states (NY, NJ, CT, RI, and DC) all have emissions profiles dominated by transportation and buildings, with less than a third of their emissions coming from the industrial and electric power sectors. From a policy perspective, these varying sectoral emissions profiles highlight the necessity of developing sector-specific mitigation plans that focus on reducing emissions from the most important emitting sectors in each state or urban area.

The growing role of urban and state governments as leaders on U.S. climate policy underscores the urgent need to reduce uncertainties in local emissions estimates. While the development of high-resolution gridded inventories such as ACES has heretofore been driven mainly to support atmospheric modeling of the carbon cycle, they are increasingly being recognized as providing considerable value to policymakers at subnational scales (Duren & Miller, 2012; Gurney et al., 2015; Hutyra et al., 2014). In particular, the within -state and within -city spatial patterns of emissions provide information about internal variability in emissions that is almost universally absent from the official emissions inventories conducted by states and municipal governments. Many cities and states have climate action plans that set sector-specific goals for emissions reductions. While for some sectors, such as power generation, it may be sufficient to implement mitigation policies that are uniform across an urban- or state-scale spatial domain, for sectors such on-road or buildings (residential/commercial/industrial), it is expected that policies will need to be sensitive to the spatial variations of the emissions-generating activities in these sectors (i.e., traffic patterns and vehicle activity across a range of road types and sizes, energy consumption across a range of building types, and neighborhood population densities). A bottom-up inventory such as ACES that resolves these spatial variations in emissions using the most relevant and resolved spatial proxies (such as the road-level traffic volumes used in DARTE) provides urban governments with the means to benchmark existing emissions patterns, to identify locations for specific policy targeting, and the ability to evaluate changes in emissions over time within the city.

In this study we have demonstrated that the existing global-scale inventories of $FFCO_2$ emissions are clearly not suitable for regional- or urban-scale emissions validation, planning analysis, or mitigation policy decision support, despite their frequent use in such applications. Large discrepancies at regional and local scales confirm that global inventories do not accurately capture the underlying spatiotemporal patterns of source activities that drive regional and urban emissions. Bottom-up inventories, such as ACES, offer the necessary spatial fidelity to identify the dominant, sector-specific sources of carbon emissions across these highly heterogeneous landscapes; this information will be critical to provide data-driven support for policymakers within a robust national carbon monitoring system.

5. Conclusions and Future Research Needs

Large uncertainties among existing $FFCO_2$ inventories present a significant obstacle for the development and implementation of emissions reductions strategies at all levels of government. These uncertainties are particularly critical at urban scales, as over 600 cities globally have already signed on to the Global Covenant of Mayors, which commits them to significant reductions in their local greenhouse gas emissions. For the United States, the only currently available bottom-up inventory of $FFCO_2$ emissions that covers more than a single urban area is the Vulcan Project (Gurney et al., 2009), which only reports emissions for the year 2002. While groundbreaking at the time of its development, Vulcan is now over a decade out of date, and though it is still widely used, it no longer reflects the state of current U.S. emissions (Figure S8). The ACES

inventory provides up-to-date estimates of surface carbon fluxes at a higher spatial resolution than Vulcan for one of the most emissions intensive regions of the U.S., with a consistent methodology that allows for urban-scale emissions benchmarking and comparison across all municipalities and states within the ACES domain.

In the absence of an up-to-date national-level inventory with sufficient detail for their purposes, many cities and states with the need to quantify their emissions have previously been forced to create their own bespoke inventories. While the largest U.S. cities may have sufficient resources to perform this task in house, many smaller- and medium-size cities lack the resources or expertise to generate $FFCO_2$ estimates of the necessary quality. Previously, where the interests of the local research community have aligned, new urban-scale inventories have been developed for cities such as Los Angeles, CA, Salt Lake City, UT, Indianapolis, IN, and Boston, MA (Decina et al., 2016; Feng et al., 2016; Gately et al., 2017; Gurney et al., 2012; Patarasuk et al., 2016). However, all of these efforts have relied on different methodologies and data sources and are limited to small geographic domains. Evaluating the uncertainty in these individual estimates has also been difficult, as they cannot be compared to a current national or regional inventory that has been constructed in a consistent fashion from similar local-scale data. We have shown that when compared to ACES, downscaled global $FFCO_2$ inventories do not accurately capture the spatial patterns of emissions at urban scales. Leveraging the increasingly available sources of local data on emissions generating activities can reduce these large uncertainties, and the ACES inventory provides the framework for a consistent, frequently updated, high-resolution carbon monitoring system for the United States.

Given the rapid development of inverse atmospheric modeling tools, satellite observations, and a strong political will at regional and urban scales, the time is ripe for next-generation carbon monitoring systems. Future operationalization of bottom-up gridded inventories within a national CMS will require improvements across many additional government and institutional systems in order to streamline data production and acquisition. An effective CMS should integrate (1) data from the rapidly growing network of surface-, air-, and space-based atmospheric greenhouse gas measurements, (2) state-of-the-art continental and mesoscale atmospheric transport models, and (3) regularly updated, sector-specific, high-resolution estimates of $FFCO_2$ emissions. Together, these three major components of a CMS can provide vital data on emissions patterns and trends to both the research and policy communities from the national down to the local scale. Fundamental actions on climate policy in the United States over the next decade will be critically affected by whether or not the research and policy communities can succeed in developing and operationalizing a robust national carbon monitoring system. Reductions in inventory uncertainty, as demonstrated by ACES, will play a key role in improving the quality of this national CMS.

Acknowledgments
We thank Jackie Getson for technical assistance in the creation of this inventory, along with Andrew Trlica. We are also grateful for useful discussions and feedback from Kevin Gurney, Ian Sue Wing, and Andrew Reinmann. This manuscript was greatly improved by the reviews of Tomohiro Oda. This research was supported primarily by the National Aeronautics and Space Administration Carbon Monitoring System program (grants NNH13CK02C and NNX16AP23G) with additional support from National Oceanic and Atmospheric Administration (NOAA NA14OAR4310179). The data reported in this paper will be publically available at the Oak Ridge Data Active Archive Center (https://doi.org/10.3334/ORNLDAAC/1501).

References

Andres, R. J., Marland, G., Fung, I., & Matthews, E. (1996). A 1° × 1° distribution of carbon dioxide emissions from fossil fuel consumption and cement manufacture, 1950–1990. *Global Biogeochemical Cycles*, *10*(3), 419–429. https://doi.org/10.1029/96GB01523

Andres, R. J., Boden, T. a., Bréon, F. M., Ciais, P., Davis, S., Erickson, D., … Treanton, K. (2012). A synthesis of carbon dioxide emissions from fossil-fuel combustion. *Biogeosciences*, *9*(5), 1845–1871. https://doi.org/10.5194/bg-9-1845-2012

Andres, R. J., Boden, T. A., & Higdon, D. (2014). A new evaluation of the uncertainty associated with CDIAC estimates of fossil fuel carbon dioxide emission. *Tellus B*, *66*(1), 23616. https://doi.org/10.3402/tellusb.v66.23616

Asefi-Najafabady, S., Rayner, P. J., Gurney, K. R., McRobert, A., Song, Y., Coltin, K., … Baugh, K. (2014). A multiyear, global gridded fossil fuel CO_2 emission data product: Evaluation and analysis of results. *Journal of Geophysical Research: Atmospheres*, *119*, 10,213–10,231. https://doi.org/10.1002/2013JD021296

Boden, T. A., Marland, G., & Andres, R. J. (2017). *Global, Regional, and National Fossil-Fuel CO_2 Emissions. Carbon Dioxide Information Analysis Center*. Oak Ridge, Tenn., U.S.A: Oak Ridge National Laboratory, U.S. Department of Energy. https://doi.org/10.3334/CDIAC/00001_V2017

Brioude, J., Angevine, W. M., Ahmadov, R., Kim, S. W., Evan, S., McKeen, S. A., … Trainer, M. (2013). Top-down estimate of surface flux in the Los Angeles basin using a mesoscale inverse modeling technique: Assessing anthropogenic emissions of CO, NO_x and CO_2 and their impacts. *Atmospheric Chemistry and Physics*, *13*(7), 3661–3677. https://doi.org/10.5194/acp-13-3661-2013

Ciais, P., Dolman, A. J., Bombelli, A., Duren, R., Peregon, A., Rayner, P. J., … Obersteiner, M. (2014). Current systematic carbon-cycle observations and the need for implementing a policy-relevant carbon observing system. *Biogeosciences*, *11*(13), 3547–3602. https://doi.org/10.5194/bg-11-3547-2014

City of New York (2011). *Inventory of New York City Greenhouse Gas Emissions, September 2011, by Jonathan Dickinson and Andrea Tenorio*. New York, NY: Mayor's Office of Long-Term Planning and Sustainability.

City of New York (2012). Inventory of New York City greenhouse gas emissions, December 2012, by Jonathan Dickinson, Jamil Khan, Douglas Price, Steven A. Caputo, Jr. and Sergej Mahnovski. Mayor's Office of Long-Term Planning and Sustainability, New York, NY.

City of New York (2015). *New York City's Roadmap to 80 × 50*. New York: Mayor's Office of Long-Term Planning and Sustainability.

Decina, S. M., Hutyra, L. R., Gately, C. K., Getson, J. M., Reinmann, A. B., Short Gianotti, A. G., & Templer, P. H. (2016). Soil respiration contributes substantially to urban carbon fluxes in the greater Boston area. *Environmental Pollution*, *212*, 433–439. https://doi.org/10.1016/j.envpol.2016.01.012

Duren, R. M., & Miller, C. E. (2012). Measuring the carbon emissions of megacities. *Nature Climate Change*, *2*(8), 560–562. https://doi.org/10.1038/nclimate1629

Engelen, R. J., Denning, A. S., & Gurney, K. R. (2002). On error estimation in atmospheric CO_2 inversions. *Journal of Geophysical Research*, *107*(D22), 4635. https://doi.org/10.1029/2002JD002195

Federal Highway Administration (2017). *Highway Performance Monitoring System Field Manual, Chapter 6*. Washington, DC: US Department of Transportation. Retrieved from https://www.fhwa.dot.gov/policyinformation/hpms/fieldmanual/

Feng, S., Lauvaux, T., Newman, S., Rao, P., Ahmadov, R., Deng, A., … Yung, Y. L. (2016). Los Angeles megacity: A high-resolution land–atmosphere modelling system for urban CO_2 emissions. *Atmospheric Chemistry and Physics*, *16*(14), 9019–9045. https://doi.org/10.5194/acp-16-9019-2016

Gately, C. K., Hutyra, L. R., Wing, I. S., & Brondfield, M. N. (2013). A bottom up approach to on-road CO_2 emissions estimates: Improved spatial accuracy and applications for regional planning. *Environmental Science & Technology*, *47*(5), 2423–2430. https://doi.org/10.1021/es304238v

Gately, C. K., Hutyra, L. R., & Sue Wing, I. (2015). Cities, traffic, and CO_2: A multidecadal assessment of trends, drivers, and scaling relationships. *Proceedings of the National Academy of Sciences*, *112*(16), 4999–5004. https://doi.org/10.1073/pnas.1421723112

Gately, C. K., Hutyra, L. R., Peterson, S., & Sue Wing, I. (2017). Urban emissions hotspots: Quantifying vehicle congestion and air pollution using mobile phone GPS data. *Environmental Pollution*, *229*, 496–504. https://doi.org/10.1016/j.envpol.2017.05.091

Geels, C., Doney, S. C., Dargaville, R., Brandt, J., & Christensen, J. H. (2004). Investigating the sources of synoptic variability in atmospheric CO_2 measurements over the Northern Hemisphere continents: A regional model study. *Tellus B*, *56*(1), 35–50. https://doi.org/10.3402/tellusb.v56i1.16399

Global Covenant of Mayors for Climate and Energy (2016), http://www.covenantofmayors.eu/about/covenant-of-mayors_en.html

Gregg, J. S., Andres, R. J., & Marland, G. (2008). China: Emissions pattern of the world leader in CO_2 emissions from fossil fuel consumption and cement production. *Geophysical Research Letters*, *35*, L08806. https://doi.org/10.1029/2007GL032887

Gregg, J. S., Losey, L. M., Andres, R. J., Blasing, T. J., & Marland, G. (2009). The temporal and spatial distribution of carbon dioxide emissions from fossil-fuel use in North America. *Journal of Applied Meteorology and Climatology*, *48*(12), 2528–2542. https://doi.org/10.1175/2009JAMC2115.1

Gurney, K. R., Law, R. M., Denning, A. S., Rayner, P. J., Baker, D., Bousquet, P., … Yuen, C.-W. (2003). TransCom 3 CO_2 inversion intercomparison: 1. Annual mean control results and sensitivity to transport and prior flux information. *Tellus B*, *55*(2), 555–579. https://doi.org/10.3402/tellusb.v55i2.16728

Gurney, K. R., Chen, Y. H., Maki, T., Kawa, S. R., Andrews, A., & Zhu, Z. X. (2005). Sensitivity of atmospheric CO_2 inversions to seasonal and interannual variations in fossil fuel emissions. *Journal of Geophysical Research*, *110*, D10308. https://doi.org/10.1029/2004JD005373

Gurney, K., Mendoza, D., Zhou, Y., Fisher, M., Miller, C., Geethakumar, S., & De La Rue Dy Can, S. (2009). High resolution fossil fuel combustion emission fluxes for the United States. *Environmental Science & Technology*, *43*(14), 5535–5541. https://doi.org/10.1021/es900806c

Gurney, K., Mendoza, D., Zhou, Y., Fisher, M., Miller, C., Geethakumar, S., & De La Rue Dy Can, S. (2010). Vulcan science methods documentation, version 2.0. Retrieved from http://vulcan.project.asu.edu/pdf/Vulcan.documentation.v2.0.online.pdf, (Accessed on September 1, 2015).

Gurney, K. R., Razlivanov, I., Song, Y., Zhou, Y., Benes, B., & Abdul-Massih, M. (2012). Quantification of fossil fuel CO_2 emissions on the building/street scale for a large U.S. City. *Environmental Science & Technology*, *46*(21), 12,194–12,202. https://doi.org/10.1021/es3011282

Gurney, K. R., Romero-Lankao, P., Seto, K. C., Hutyra, L. R., Duren, R. M., Kennedy, C., … Sperling, J. (2015). Track urban emissions on a human scale. *Nature*, *525*(7568), 179–181. https://doi.org/10.1038/525179a

Gurney, K. R., Huang, J., & Coltin, K. (2016). Bias present in US federal agency power plant CO_2 emissions data and implications for the US clean power plan. *Environmental Research Letters*, *11*(6), 64005. https://doi.org/10.1088/1748-9326/11/6/064005

Hakkarainen, J., Ialongo, I., & Tamminen, J. (2016). Direct space-based observations of anthropogenic CO_2 emission areas from OCO-2. *Geophysical Research Letters*, *43*(21), 11,400–11,406. https://doi.org/10.1002/2016GL070885

Hardiman, B. S., Wang, J. A., Hutyra, L. R., Gately, C. K., Getson, J. M., & Friedl, M. A. (2017). Accounting for urban biogenic fluxes in regional carbon budgets. *Science of the Total Environment*, *592*, 366–372. https://doi.org/10.1016/j.scitotenv.2017.03.028

Hogue, S., Marland, E., Andres, R. J., Marland, G., & Woodard, D. (2016). Uncertainty in gridded CO_2 emissions estimates. *Earth's Future*, *4*(5), 225–239. https://doi.org/10.1002/2015EF000343

Hutchins, M. G., Colby, J. D., Marland, G., & Marland, E. (2016). A comparison of five high-resolution spatially-explicit, fossil-fuel, carbon dioxide emission inventories for the United States. *Mitigation and Adaptation Strategies for Global Change*, *22*(6), 1–26.

Hutyra, L. R., Duren, R., Gurney, K. R., Grimm, N., Kort, E. A., Larson, E., & Shrestha, G. (2014). Urbanization and the carbon cycle: Current capabilities and research outlook from the natural sciences perspective. *Earth's Future*, *2*(10), 473–495. https://doi.org/10.1002/2014EF000255

Intergovernmental Panel on Climate Change (2013). *Climate Change 2013: The Physical Science Basis. Contribution of Working Group I to the Fifth Assessment Report of the Intergovernmental Panel on Climate Change*, In T. F. Stocker, et al. (Eds.), (1535 pp.). Cambridge, U. K., and New York: Cambridge University Press. https://doi.org/10.1017/CBO9781107415324

Jones, C., & Kammen, D. M. (2014). Spatial distribution of U.S. household carbon footprints reveals suburbanization undermines greenhouse gas benefits of urban population density. *Environmental Science & Technology*, *48*(2), 895–902. https://doi.org/10.1021/es4034364

Lauvaux, T., Miles, N. L., Deng, A., Richardson, S. J., Cambaliza, M. O., Davis, K. J., … Wu, K. (2016). High-resolution atmospheric inversion of urban CO_2 emissions during the dormant season of the Indianapolis flux experiment (INFLUX). *Journal of Geophysical Research: Atmospheres*, *121*, 5213–5236. https://doi.org/10.1002/2015JD024473

Macknick, J. (2014). Energy and CO_2 emission data uncertainties. https://doi.org/10.4155/CMT.11.10

Marcotullio, P. J., Sarzynski, A., Albrecht, J., & Schulz, N. (2012). The geography of urban greenhouse gas emissions in Asia: A regional analysis. *Global Environmental Change*, *22*(4), 944–958. https://doi.org/10.1016/j.gloenvcha.2012.07.002

Marland, G., Rotty, R. M., & Treat, N. L. (1985). CO_2 from fossil fuel burning: Global distribution of emissions. *Tellus*, *37B*(4–5), 243–258. https://doi.org/10.1111/j.1600-0889.1985.tb00073.x

McDonald, B., McBride, Z., Martin, E. W., & Harley, R. (2014). A high-resolution mapping of motor vehicle carbon dioxide emissions. *Journal of Geophysical Research: Atmospheres*, *119*, 5283–5298. https://doi.org/10.1002/2013JD021219

McKain, K., Wofsy, S. C., Nehrkorn, T., Eluszkiewicz, J., Ehleringer, J. R., & Stephens, B. B. (2012). Assessment of ground-based atmospheric observations for verification of greenhouse gas emissions from an urban region. *Proceedings of the National Academy of Sciences*, *109*(22), 8423–8428. https://doi.org/10.1073/pnas.1116645109

Mckain, K., Down, A., Raciti, S. M., Budney, J., Hutyra, L. R., & Floerchinger, C. (2014). Methane emissions from natural gas infrastructure and use in the urban region of Boston, Massachusetts. *Proceedings of the National Academy of Sciences*, *112*(7), 1941–1946.

Mendoza, D., Gurney, K. R., Geethakumar, S., Chandrasekaran, V., Zhou, Y., & Razlivanov, I. (2013). Implications of uncertainty on regional CO2 mitigation policies for the U.S. onroad sector based on a high-resolution emissions estimate. *Energy Policy*, *55*, 386–395. https://doi.org/10.1016/j.enpol.2012.12.027

Metropolitan Area Planning Council (2014). Massachusetts land parcel database. Retrieved from http://www.mapc.org/parceldatabase; (Accessed on June 10, 2016).

Miller, S. M., & Michalak, A. M. (2016). Constraining sector-specific CO_2 and CH_4 emissions in the United States. *Atmospheric Chemistry and Physics Discussions*, *0*, 1–33. https://doi.org/10.5194/acp-2016-643

National Research Council (2009). Driving and the built environment: The effects of compact development on motorized travel, energy use, and CO_2 emissions. Committee for the Study on the Relationships Among Development Patterns and Vehicle Miles Traveled, Transportation Research Board, and National Research Council Board on Energy and Environmental Systems, Washington, DC.

New York State Department of Environmental Conservation (2016). Data on oil, gas, and other wells in New York state. Retrieved from http://www.dec.ny.gov/energy/1603.html, (Accessed on June 10, 2016).

Oak Ridge National Laboratory (2014). *LandScan Global Population Dataset 2013*. Oak Ridge, TN: Oak Ridge National Laboratory.

Oda, T., & Maksyutov, S. (2011). A very high-resolution (1 km × 1 km) global fossil fuel CO_2 emission inventory derived using a point source database and satellite observations of nighttime lights. *Atmospheric Chemistry and Physics*, *11*(2), 543–556. https://doi.org/10.5194/acp-11-543-2011

Oda, T., Ott, L., Topylko, P., Halushchak, M., Bun, R., Lesiv, M., … Horabik-Pyzel, J. (2015). Uncertainty associated with fossil fuel carbon dioxide (CO_2) gridded emission datasets. In *Proceedings, 4th International Workshop on Uncertainty in Atmospheric Emissions, 7–9 October 2015, Krakow, Poland* (pp. 124–129). Warsaw, Poland: Systems Research Institute, Polish Academy of Sciences.

Ogle, S. M., Davis, K., Lauvaux, T., Schuh, A., Cooley, D., West, T. O., … Scott Denning, A. (2015). An approach for verifying biogenic greenhouse gas emissions inventories with atmospheric CO_2 concentration data. *Environmental Research Letters*, *10*(3), 34012. https://doi.org/10.1088/1748-9326/10/3/034012

Olivier, J. G. J. and Janssens-Maenhout, G. (2012). CO_2 emissions from fuel combustion. In CO_2 *Emissions from Fuel Combustion -- 2012 Edition, IEA* CO_2 *report 2012, Part III, Greenhouse-Gas Emissions*.

Patarasuk, R., Gurney, K. R., O'Keeffe, D., Song, Y., Huang, J., Rao, P., … Ehleringer, J. R. (2016). Urban high-resolution fossil fuel CO_2 emissions quantification and exploration of emission drivers for potential policy applications. *Urban Ecosystem*, *19*(3), 1013–1039. https://doi.org/10.1007/s11252-016-0553-1

Pennsylvania Department of Environmental Protection (2016). Pennsylvania geospatial data clearinghouse oil and gas locations. Retrieved from http://www.pasda.psu.edu/uci/DataSummary.aspx?dataset=283, (Accessed on June 10, 2016).

Peters, W., Jacobson, A. R., Sweeney, C., Andrews, A. E., Conway, T. J., Masarie, K., … Tans, P. P. (2007). An atmospheric perspective on North American carbon dioxide exchange: CarbonTracker. *Proceedings of the National Academy of Sciences*, *104*(48), 18,925–18,930. https://doi.org/10.1073/pnas.0708986104

Regional Greenhouse Gas Initiative (2005). Available at: www.rggi.org

Sarzynski, A. (2012). Bigger is not always better: A comparative analysis of cities and their air pollution impact. *Urban Studies*, *49*(14), 3121–3138. https://doi.org/10.1177/0042098011432557

Schneising, O., Heymann, J., Buchwitz, M., Reuter, M., Bovensmann, H., & Burrows, J. P. (2013). Anthropogenic carbon dioxide source areas observed from space: Assessment of regional enhancements and trends. *Atmospheric Chemistry and Physics*, *13*(5), 2445–2454. https://doi.org/10.5194/acp-13-2445-2013

Schuh, A. E., Denning, A. S., Corbin, K. D., Baker, I. T., Uliasz, M., Parazoo, N., … Worthy, D. E. J. (2010). A regional high-resolution carbon flux inversion of North America for 2004. *Biogeosciences*, *7*(5), 1625–1644. https://doi.org/10.5194/bg-7-1625-2010

Shiga, Y. P., Michalak, A. M., Gourdji, S. M., Mueller, K. L., & Yadav, V. (2014). Detecting fossil fuel emissions patterns from subcontinental regions using North American in situ CO_2 measurements. *Geophysical Research Letters*, *41*, 4381–4388. https://doi.org/10.1002/2014GL059684

State of California AB-32 (2006). California global warming solutions act, health & SC § 38500–38598.

Tohjima, Y., Kubo, M., Minejima, C., Mukai, H., Tanimoto, H., Ganshin, A., … Kita, K. (2014). Temporal changes in the emissions of CH4 and CO from China estimated from CH_4/CO_2 and CO/CO_2 correlations observed at Hateruma Island. *Atmospheric Chemistry and Physics*, *14*(3), 1663–1677. https://doi.org/10.5194/acp-14-1663-2014

Turnbull, J. C., Tans, P. P., Lehman, S. J., Baker, D., Conway, T. J., Chung, Y. S., … Zhou, L.-X. (2011). Atmospheric observations of carbon monoxide and fossil fuel CO_2 emissions from East Asia. *Journal of Geophysical Research*, *116*, D24306. https://doi.org/10.1029/2011JD016691

Turnbull, J. C., Sweeney, C., Karion, A., Newberger, T., Lehman, S. J., Tans, P. P., … Razlivanov, I. (2015). Toward quantification and source sector identification of fossil fuel CO_2 emissions from an urban area: Results from the INFLUX experiment. *Journal of Geophysical Research: Atmospheres*, *120*, 292–312. https://doi.org/10.1002/2014JD022555

United Nations (2012). World urbanization prospects, the 2011 revision: Highlights, United Nations Department of economic and social affairs, Population Division, New York, NY. Retrieved from www.un.org/en/development/desa/publications/ world-urbanization-prospects-the-2011-revision.html, (Accessed June 01, 2015).

United Nations (2014). 2013 energy statistics yearbook, United Nations Department for economic and social information and policy analysis, Statistics Division, New York, NY.

United States Census Bureau (2015). American community survey 5-year estimates 2010-2014, table B25040 house heating fuel by Census Block Group. Retrieved from http://factfinder.census.gov, (Accessed on June 10, 2016).

United States Census Bureau, Center for Economic Studies (2014). Longitudinal employer-household dynamics. Retrieved from http://lehd.ces.census.gov/data (Accessed on June 10, 2016).

United States Environmental Protection Agency (2008). Regulatory impact analysis—Control of emissions of air pollution from locomotive engines and marine compression ignition engines less than 30 liters per cylinder (Report No. EPA420-R-08-001a). Washington, DC. Retrieved from http://www.epa.gov/otaq/regs/nonroad/420r08001a.pdf, (Accessed on September 1, 2015).

United States Environmental Protection Agency (2009a). Office of transportation and air quality. Emission Factors for Locomotives Report: EPA-420-F-09-025, Tables 1,2,3. Washington, DC.

United States Environmental Protection Agency (2009b). Current methodologies in preparing mobile source port-related emission inventories final report, Washington, DC.

United States Environmental Protection Agency (2014a). The 2011 National Emissions Inventory. Retrieved from https://www.epa.gov/air-emissions-inventories/2011-national-emissions-inventory-nei-data, (Accessed on June 10, 2016).

United States Environmental Protection Agency (2014b). Greenhouse gas reporting program. Retrieved from https://www.epa.gov/ghgreporting, (Accessed on June 10, 2016).

United States Environmental Protection Agency (2014c). Technology transfer network, clearinghouse for inventories and emissions factors, WEBFire emissions factor database. Retrieved from https://www3.epa.gov/ttn/chief/webfire/index.html, (Accessed on June 10, 2016).
Virginia Department of Mines, Minerals, and Energy (2016). Division of gas and oil data information system. Retrieved from https://www.dmme.virginia.gov/dgoinquiry/, (Accessed on June 10, 2016).
Vogel, F. R., Ishizawa, M., Chan, E., Chan, D., Hammer, S., Levin, I., & Worthy, D. E. J. (2012). Regional non-CO_2 greenhouse gas fluxes inferred from atmospheric measurements in Ontario, Canada. *Journal of Integrative Environmental Sciences*, *9*(sup1), 41–55. https://doi.org/10.1080/1943815X.2012.691884
West Virginia Department of Environmental Protection (2016). Office of oil and gas well locations. Retrieved from http://tagis.dep.wv.gov/oog/, (Accessed on June 10, 2016).
Wu, L., Bocquet, M., Lauvaux, T., Chevallier, F., Rayner, P., & Davis, K. (2011). Optimal representation of source-sink fluxes for mesoscale carbon dioxide inversion with synthetic data. *Journal of Geophysical Research*, *116*, D21304. https://doi.org/10.1029/2011JD016198
Wunch, D., Wennberg, P. O., Toon, G. C., Keppel-Aleks, G., & Yavin, Y. G. (2009). Emissions of greenhouse gases from a North American megacity. *Geophysical Research Letters*, *36*, L15810. https://doi.org/10.1029/2009GL039825
Yadav, V., Michalak, A. M., Ray, J., & Shiga, Y. P. (2016). A statistical approach for isolating fossil fuel emissions in atmospheric inverse problems. *Journal of Geophysical Research: Atmospheres*, *121*, 12,490–12,504.https://doi.org/10.1002/2016JD025642
Zhang, X., Gurney, K. R., Rayner, P., Liu, Y., & Asefi-Najafabady, S. (2014). Sensitivity of simulated CO_2 concentration to regridding of global fossil fuel CO_2 emissions. *Geoscientific Model Development*, *7*(6), 2867–2874. https://doi.org/10.5194/gmd-7-2867-2014